High-Throughput Screening for Kv1.3 Channel Blockers Using an Improved FLIPR-Based Membrane-Potential Assay

Kun Liu, Manoj Samuel, Jeff Tillett, James K. Hennan, Belew Mekonnen, Veronica Soloveva, Richard K. Harrison, Jeff W. Paslay and James Larocque

J Biomol Screen 2010 15: 185 originally published online 31 December 2009
DOI: 10.1177/1087057109356209

High-Throughput Screening for Kv1.3 Channel Blockers Using an Improved FLIPR-Based Membrane-Potential Assay

KUN LIU,[1] MANOJ SAMUEL,[1] JEFF TILLETT,[2] JAMES K. HENNAN,[3] BELEW MEKONNEN,[4] VERONICA SOLOVEVA,[1] RICHARD K. HARRISON,[1] JEFF W. PASLAY,[1] and JAMES LAROCQUE[1]

Voltage-gated K^+ channels are potential drug targets for an increasing number of disease indications. Searching for compounds that modulate K^+ channel activities by high-throughput screening (HTS) is becoming a standard approach in the drug discovery effort. Here the authors report an improved fluorometric imaging plate reader (FLIPR) membrane potential assay for Kv1.3 K^+ channel HTS. They have found that the Chinese hamster ovary (CHO) cells have endogenous membrane electrogenic transporters that contribute to maintaining membrane potential. Blocking the recombinant K^+ channels in the overexpressing CHO cell line hardly changed the membrane potential. Inhibition of the endogenous transporters is essential to achieve the required assay robustness. The authors identified the optimal assay conditions and designed a simple assay format. After an HTS campaign using this assay, various chemical series of Kv1.3 channel blockers have been identified and confirmed by the automated electrophysiological IonWorks assay. The correlation in dose response between FLIPR and IonWorks was established by biophysical modeling and experimental data. After characterization using patch-clamp recording, both use-dependent and use-independent compounds were identified. Some compounds possess nanomolar potency, indicating that the FLIPR assay is effective for successfully identifying K^+ channel blockers as novel drug candidates. (*Journal of Biomolecular Screening* 2010:185-195)

Key words: high-throughput screening, Kv1.3 channel, FLIPR membrane potential assay, sodium azide, IonWorks

INTRODUCTION

VOLTAGE-GATED ION CHANNELS REPRESENT A MAJOR FAMILY of therapeutic targets for a variety of disease indications due to the important functions in physiological processes. A member of mammalian "Shaker" family channels, Kv1.3 has been identified as a major K^+ channel type expressed in immune cells, including T and B cells, and considered a potential drug target for autoimmune diseases.[1-7] Recently, studies have also showed that Kv1.3 channel knockout mice have lean body weight and prolonged life span, preferentially caused by an increase in insulin sensitivity in adipocytes.[8,9] Therefore, Kv1.3 channel blockers could be potentially used as antidiabetic agents. Searching for compounds that block Kv1.3 channel activities has started for years, and a number of blockers have been reported with the chemical entities from toxins to small molecules. However, the clinical development has not yet been successful, mostly due to the difficulty in achieving selectivity of the action. Therefore, screening a large compound library for expanded chemical entities would provide increased opportunities to improve compound properties and to achieve clinically viable agents.

High-throughput screening (HTS) has been demonstrated as a highly valuable approach in drug discovery. Typically, a compound library containing half to 1 million compounds is screened against each desirable target. Tens of thousands of the hits are identified for follow-up assessment. This approach requires development of HTS-adaptable assays that provide effective throughput to complete the screen in a practical length of time. For ion channel assays, the conventional electrophysiological technique is still considered a gold standard in terms of data quality and specificity, but the throughput of the assay is too low to be suitable for HTS. Although the recently developed automated patch clamp has greatly improved throughput, the application of such assays in HTS format is still impractical. As a fluorescence-based assay, fluorometric imaging plate reader (FLIPR) has been commonly used for HTS as a functional assay format for G-protein-coupled receptors (GPCR) and ion channels. FLIPR is an imaging-based assay system with automated liquid handling capable of generating 20,000 to 50,000 data points per day. In the past decade, a variety of FLIPR suitable fluorescent dyes have been developed and applied to HTS campaigns.[10-17] For potassium channel assays, membrane-potential dye was widely employed based on the principles that inhibition of K^+ channel activity would cause

[1]Department of Screening Sciences, [2]Department of Cardiovascular and Metabolic Diseases, [3]Project Management, and [4]Department of Medicinal Chemistry, Wyeth Research, Collegeville, Pennsylvania

Received Aug 21, 2009, and in revised form Oct 9, 2009; Accepted for publication Oct 30, 2009

Journal of Biomolecular Screening 15(2); 2010
DOI: 10.1177/1087057109356209

changes in membrane potential. K^+ channel functions are physiologically associated with membrane potential in either excitable or nonexcitable cells. Using the membrane-potential assay to assess K^+ channel activity should be physiologically relevant, outweighing the assays using Rb^+ or Tl^+ as carriers.[18-20] However, membrane potential is an essential property for almost every type of living cells, maintained by not only K^+ channel function but also other membrane transporters. These non–K^+ channel mechanisms would interfere with membrane-potential signal in the assay and largely reduce the assay performance, which therefore hindered the assay application. To surmount the obstacle, the previous applications used K^+ channel openers or high concentration of K^+ to induce membrane-potential change and then examined the compound effect on this signal.[16,21] One endpoint assay previously described for Kv1.3 channel was performed at temperatures below 2°C.[22,23] The nonphysiological conditions used in these assays are subject to modifying channel properties, and thus the assay may misinterpret the compound activities. The low-temperature assay requirement is also a challenge for the HTS campaign to adapt. Therefore, it is necessary to develop a simple, reliable, and robust assay that can be performed under physiologically relevant conditions.

In this study, we report a robust membrane-potential assay for Kv1.3 channel HTS. We have identified the issues for establishing this physiologically relevant format and found solutions to achieve the assay robustness. We have also generated a model to correlate the results of this assay with an electrophysiological approach. The assay was successfully applied to the HTS campaign. The primary hits were confirmed by the follow-on electrophysiological screening. The Kv1.3 channel blockers with good potency were identified and confirmed by the next level of assessment.

MATERIALS AND METHODS

Media and chemicals

Cell culture medium: Ham's F-12 (Cellgro, Manassas, VA) supplemented with 10% fetal bovine serum (FBS; heat inactivated, Invitrogen, Carlsbad, CA), 100 µg/mL streptomycin, 100 U/mL penicillin (Invitrogen), and 200 µg/mL Geneticin

IonWorks internal solution: 140 mM KCl, 2 mM $MgCl_2$, 5 mM EGTA, and 10 mM HEPES (pH 7.2)

IonWorks external solution: DPBS containing calcium and magnesium buffer (Invitrogen)

Patch-clamp pipette solution: 140 mM KCl, 4 mM $MgCl_2$, 10 mM EGTA, and 10 mM HEPES (pH 7.2)

Patch-clamp external solution: 135 mM NaCl, 5 mM KCl, 1 mM $CaCl_2$, 1.17 mM $MgSO_4$, and 10 mM HEPES (pH 7.4)

All chemicals and compounds were purchased from Sigma-Aldrich (St. Louis, MO) unless otherwise mentioned. Psora-4 was dissolved in DMSO at 10 mM as stock and margatoxin was reconstituted according to the manufacturer's protocol.

Cell culture

The Chinese hamster ovary (CHO) cells stably expressing Kv1.3 (CHO-Kv1.3) and Kv1.5 channels (CHO-Kv1.5) were purchased from Aurora Biomed (Vancouver, BC, Canada) and Millipore (Billerica, MA), respectively. Cells were maintained in the culture medium to 80% to 90% of confluence and plated in 96-well clear-bottom black plates at a density of 50,000/well or in poly-D-lysine (PDL)–coated 384-well clear-bottom plates (VWR International, West Chester, PA) at a density of 15,000/well. After overnight incubation at 37°C with 95/5% air/CO_2, the plate was used for FLIPR assay. For IonWorks and patch-clamp studies, cells were split into 35-mm culture dishes and incubated for 24 to 72 h before use. The HTS was conducted using a large bulk of frozen cells with a fresh vial of cells being thawed and consistently cultured for each day of screening.[24] The cells were cultured, split to expand, harvested, counted, and plated using a TAP SelecT automated cell culture system (The Automation Partnership, Royston, UK).

FLIPR membrane-potential assay

FLIPR assay development was performed in accordance with the manufacturer's protocol (Molecular Devices, Sunnyvale, CA). Briefly, cell plates were loaded with assay buffer containing 1× membrane-potential dye component A. After a 40-min incubation at room temperature, the plates were placed on the platform of FLIPR384 (Molecular Devices), and the fluorescence was read with excitation/emission at 488/540 nm.

The HTS campaign was conducted using a fully automated High-Speed Distributed Motion (HSDM) Thermo LAS microplate assay system with dual FLIPR Tetras previously described.[24] The FLIPR assay was performed in 384-well plates as described above on batches of up to 189 plates prepared and incubated, with lids, overnight on the TAP SelecT cell culture system. Nine racks with each of 21 plates were transferred from the SelecT incubator to the assay system incubator for storage at 37°C 5% CO_2 prior to use. The assay system, based on a predetermined 12-h schedule set to achieve uniform and consistent plate handling, retrieves each plate from the incubator and removes its lid temporarily for processing. The plates are washed with 70 µL of assay buffer, leaving 25 µL behind and loaded with 40 µL of assay buffer containing 1.2× membrane-potential dye component A and 10 mM NaN_3, followed by the addition of 10 µL of test compound, control compound, or assay buffer. The system re-lids each plate and incubates it for 60 min at room temperature with 5% CO_2 in a second incubator. The plates are then retrieved from the incubator, de-lidded, and transferred to one of the FLIPR Tetras for an endpoint fluorescence determination. Data are presented in either relative fluorescence unit (RFU) or logarithm of fold induction (FI) normalized by the RFU values from control (buffer-treated) wells.

IonWorks electrophysiological assay

Kv1.3 current was recorded on the CHO-Kv1.3 cells using IonWorks Quattro (Molecular Devices) platform in high-throughput (HT) mode. Cells were maintained in regular culture condition and harvested freshly before assay. Versene (Invitrogen) was used as dissociation buffer to make suspension cells at a density of 5×10^5/mL before being loaded into the platform. IonWorks recording was conducted following the manufacturer's protocol (Molecular Devices). As soon as the seal was achieved, the internal solution containing 0.1 mg/mL Amphotericin B was applied to make perforated whole-cell configuration. Voltage-dependent Kv1.3 current was evoked by double depolarization pulses from holding potential at –70 to 30 mV for 1 s in 1-s intervals. The compound effect on Kv1.3 channel activity was evaluated by comparing the current amplitudes at the end of the first depolarization pulse before and 3 to 5 min after the compound addition. Eight concentrations of compound starting at 30 μM in a half-logarithm dilution were used to generate 8-point dose response. The data were analyzed using XLFit4 software (IDBS Limited, Guildford, UK). IC_{50} was generated by fitting the dose-response data to the Hill equation.

Patch-clamp recording

Cells were dissociated using trypsin (0.05 mg/mL), washed once with the culture medium, and harvested into a 15-mL centrifuge tube at a density of 10^6/mL. The freshly isolated cells would be used within 4 h after preparation. High-resolution current recordings were acquired with a computer-based patch-clamp amplifier system (EPC-10; HEKA, Lambrecht, Germany). Patch pipettes had resistances between 2 and 5 MOhm after filling with the standard pipette solution. After establishing whole-cell configuration, the membrane potential was held at either –70 or –80 mV. A series of voltage protocols was used to test the voltage dependence of the channel activation. To test compound effect, we applied a single voltage pulse stepped from a holding potential at –80 to 20 mV for 1 s. Liquid junction potential, capacitive currents, and series resistance were determined and corrected using the automatic compensation of the EPC-10. Compounds were delivered through a gravity-driven perfusion system, and the effect was calculated as percent inhibition of the current amplitudes at the end of the voltage pulse. To generate a dose response, 3 to 4 concentrations starting at 20 μM in 10-fold dilution were tested. IC_{50} was generated as described for IonWorks.

Data analysis and modeling

Kv1.3 channels are mainly expressed in nonexcitable cells such as lymphocytes and adipocytes, in which the major function of those channels is to regulate resting membrane potential to affect the downstream biological processes. Kv1.3 channel blockers are expected to depolarize membrane potential in these cells. In the present study, CHO-Kv1.3 cells have no other K^+ current except substantially expressed Kv1.3 current, conferring an ideal cellular system for modeling the role of the voltage-gated K^+ channel in maintaining resting membrane potential. Assuming that the Kv1.3 channel is the only K^+ channel in the cell membrane, carrying K^+ current when it is open, the relationship of channel conductance (G_K) versus membrane voltage (V_m) should follow the Boltzmann equation:

$$G_K = G_{K0}/(1 + EXP(-k(V_m - V_{1/2}))), \quad (1)$$

where k is a constant, and $V_{1/2}$ is half-activation voltage. G_{K0} is maximal open conductance by voltage. When channel blockers are applied, G_{K0} is a function of the blocker concentration (C) described by the Hill equation:

$$G_{K0} = G_{max}/(1 + (C/IC_{50})\text{^}n), \quad (2)$$

where G_{max} is the maximal open conductance when entire channels are open without blockade; IC_{50} is the blocker concentration at 50% of channel blockade, which is derived from patch-clamp recording at maximal activation voltage; and n is the Hill coefficient. Then, the K^+ current (I_K) conducted by the K^+ conductance equals

$$I_K = G_K (V_m - V_K) = G_{max}/((1 + EXP(-k(V_m - V_{1/2})))(1 + (C/IC_{50})\text{^}n)),$$

where V_K denotes K^+ reversal potential. In the physiological condition, I_K is an outward current, which hyperpolarizes membrane potential. The hyperpolarized V_m would generate nonspecific leak current (I_{leak}) through membrane leak conductance (G_m):

$$I_{leak} = G_m \times V_m.$$

The membrane potential will stay constant when $I_K = -I_{leak}$. Combine the above equations, and then

$$G_{max}/((1 + EXP(-k(V_m - V_{1/2})))(1 + (C/IC_{50})\text{^}n)) = -G_m \times V_m.$$

Let $G_0 = G_{max}/G_m$, which denotes the ratio of the channel maximal conductance and membrane leak conductance, and then

$$C = IC_{50} (G_0 (V_K/V_m - 1)/(1 + EXP(-k(V_m - V_{1/2}))) - 1)\text{^}(1/n). \quad (3)$$

This equation represents the relationship of blocker concentrations and the membrane potential generated by the potassium channel activities.

The equation for linear fit (presented later in **Fig. 7**) is

$$y = a + b \times x,$$

where b is the slope, and x and y could be in linear or log scale. To demonstrate assay robustness, we calculated the Z′ factor according to the following equation:

$$Z' = 1 - [3*(SD_H + SD_L)/(Mean_H - Mean_L)],$$

where SD_H is the standard deviation of the high signal (channel blocker), and SD_L is the standard deviation of the low signal (buffer control). $Mean_H$ and $Mean_L$ are the averages of the high signal and low signal, respectively. Data are presented in mean ± SD. Origin 6.1® (Origin Lab Corporation, Northampton, MA) was used for all data fitting and correlation analysis.

RESULTS AND DISCUSSION

CHO cells do not have detectable voltage-dependent channel current, so they are used widely as a robust expression system for ion channel studies. Stable expression of Kv1.3 channel in CHO cells provokes large voltage-dependent K^+ current. The current can be elicited by membrane depolarization, and the significant inactivation can be observed at a membrane potential higher than –30 mV. As shown in **Figure 1A**, the voltage dependence curve represents the key properties of the Kv1.3 channel, as described in earlier studies.[4] The channel starts to activate when membrane is depolarized to more positive than –60 mV, and the activation saturates at the potential higher than –20 mV. According to classical electrophysiology theory, CHO-Kv1.3 cells will establish membrane potential by activated Kv1.3 channels. When the channel activates, the K^+ efflux current (I_K) builds potential difference, which then generates a leak current (I_{leak}). As long as I_K is greater than I_{leak}, membrane potential will be driven close to the K^+ reversal potential, at which I_K will be largely reduced until I_K equals $-I_{leak}$. At –20 mV, the current peak amplitude was 832 ± 54 pA (n = 9) in CHO-Kv1.3 cells, and the maximal K^+ conductance (reversal potential at –108 mV in the experimental condition) was 9.45 nS. The leak conductance in CHO parental cells was 0.19 nS (13 pA at –70 mV). This approximate 50-fold conductance ratio ensures that the membrane potential stays at the K^+ reversal potential. Indeed, current clamp recording showed that changes in extracellular K^+ concentration affected the membrane potential exactly as predicted by the Nernst equation when the calculated reversal potentials fell in channel activation range (**Fig. 1B,C**). However, membrane potential would not be hyperpolarized below –58 mV, at which the Kv1.3 channel would be completely closed. With regard to this observation, complete block of the channel activity by channel blockers would keep membrane potential depolarized, as shown by the dotted line in **Figure 1C**.

To develop an HTS assay, we decided to adopt a FLIPR-based membrane-potential assay because currently commercially available membrane-potential dye could achieve robust resolution for detection of changes in membrane potential. We first chose Psora-4 as our benchmark compound due to the fact that Psora-4 is so far the most potent known small-molecule

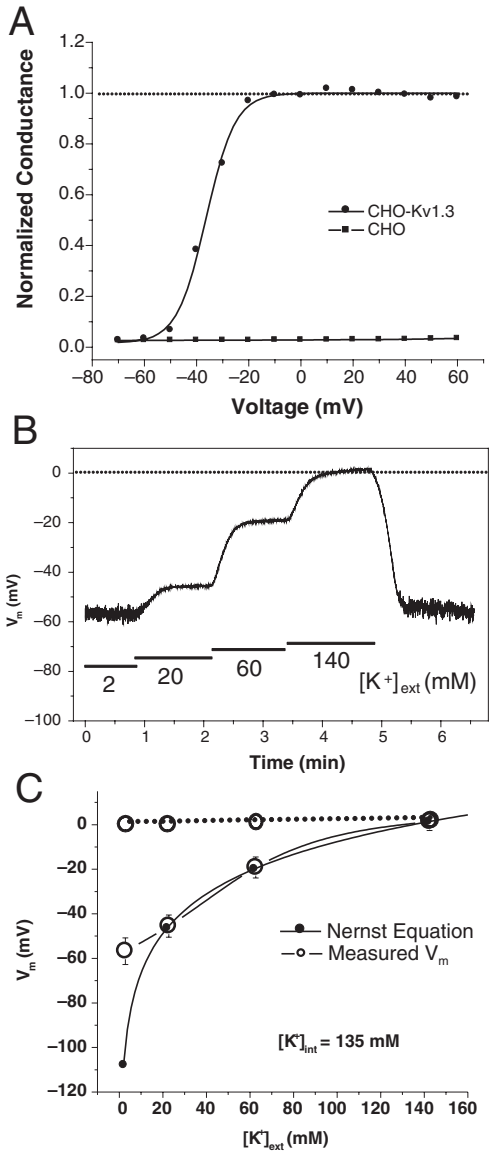

FIG. 1. Patch-clamp recording of Kv1.3 channels. CHO-Kv1.3 cells showed robust voltage-dependent current in the voltage range from –70 to 60 mV, whereas CHO parental cells showed no detectible current. (**A**) The conductance derived from tail current plotted against the voltage was fitted with the Boltzmann equation (equation 1) for CHO-Kv1.3. The fitting parameters are as follows: k = 5.97; $V_{1/2}$ = –36.5 mV. (**B**) Current clamp recording of CHO-Kv1.3 cells in the presence of various concentrations of K^+ in external solution. (**C**) Membrane potential plotted against the external K^+ concentration. The membrane-potential values were derived by the Nernst equation (solid circles) and by the current clamp recording (open circles with solid lines, n = 4). The predicted membrane-potential values at completely blocked K^+ channel activity are shown in open circles with dotted lines.

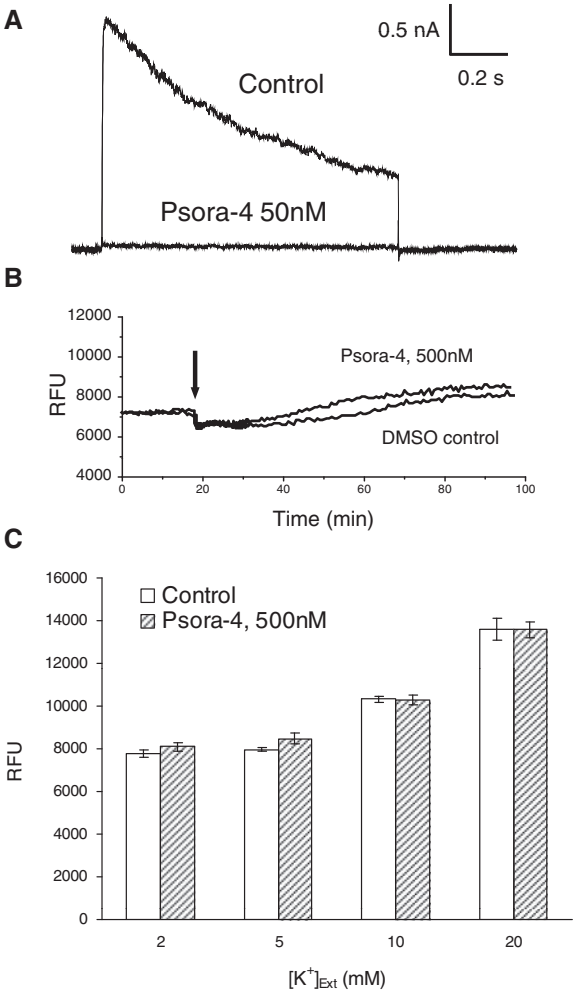

FIG. 2. Effect of Psora-4 on Kv1.3 channel current in patch-clamp recording and on membrane potential detected by fluorometric imaging plate reader (FLIPR) assay. (**A**) Psora-4 at 50 nM completely blocked Kv1.3 channel current. (**B**) Psora-4 at 500 nM slightly increased fluorescence signal in FLIPR assay. RFU, relative fluorescence unit. (**C**) Fluorescence intensities detected by FLIPR in various concentrations of external K^+ and in the presence and absence of 500 nM Psora-4. $n = 12$ for each group.

Kv1.3 blocker. We tested this compound in patch-clamp settings. As shown in **Figure 2A**, Psora-4 completely blocked the Kv1.3 channel at 50 nM. We then examined this compound in the FLIPR membrane-potential assay. As shown in **Figure 2B**, addition of Psora-4 up to 500 nM only slightly increased fluorescence signal during 80 min of recording period. Meanwhile, an increase in extracellular K^+ concentration could dramatically elevate fluorescence signal, which corresponds to the depolarization of membrane potential. This result suggests that blockade of Kv1.3 channel by Psora-4 could not depolarize membrane potential as expected. Therefore, additional mechanisms must be maintaining the membrane potential when Kv1.3 is blocked in these cells. We hypothesize that Na^+/K^+ ATPase may contribute largely to this action because CHO cells have been shown to possess profound ATPase activities.[25] We tested several ATPase antagonizing compounds and found that sodium azide (NaN_3) generated the best results. NaN_3 is an inorganic compound that antagonizes adenosine triphosphate (ATP) synthesis and reduces intracellular ATP concentration.[26] As shown in **Figure 3A**, in the presence of NaN_3, Psora-4 at 500 nM dramatically increased fluorescence response. NaN_3 induced only a slight increase in basal response. In addition, when the experiment was conducted in Cl^- free condition (replaced by aspartate), Psora-4 increased fluorescence signal at 101% with the Z′ factor at 0.63 in this representative plate. The potent Kv1.3 specific toxin blocker MgTx also induced an increase in fluorescence under the same condition. Fitting of Psora-4 and MgTx dose-dependent response with the Hill equation resulted in 39 nM and 16 nM EC_{50}s, respectively (**Fig. 3B**). The assay stability was also tested. As shown in **Figure 3C**, the robust response sustained for at least 6 h after dye loading of the cells. To rule out that the signal enhancement by NaN_3 is cell-line specific, we examined the assay condition further using the CHO-Kv1.5 stable cell line to observe the inhibition of Kv1.5 channels by Psora-4, which was previously shown to block Kv1.5 as well.[27] As shown in **Figure 4A**, Psora-4 induced a greater than 100% increase in fluorescence in the presence of 10 mM NaN_3 and the absence of Cl^-, compared to a very minimal increase in the control buffer condition. However, in CHO parental cells, both Psora-4 and MgTx did not evoke any significant changes under the same condition (**Fig. 4B**), indicating that the increase in fluorescence signal in CHO-Kv1.3 and CHO-Kv1.5 cells is an event specific to the inhibition of the overexpressed K^+ channels.

In patch-clamp recording, Psora-4 and MgTx blocked the Kv1.3 channel with IC_{50}s at 2 nM and 0.11 nM, respectively.[27,28] However, both compounds modified membrane potential at much higher EC_{50}s (**Fig. 3B**). We wanted to determine whether this discrepancy reflected other components involved in membrane-potential determination other than the Kv1.3 channel block. We tried to model the membrane-potential response to the concentration of the specific blockers based on the kinetics of the channel activation and the compound blockade (see Materials and Methods). As shown in **Figure 5**, the modeled responses to both Psora-4 and MgTx match the data obtained from FLIPR experiments tightly. The model was created based on the presumption that the Kv1.3 channel provides the only driving force for maintaining membrane potential in this system. The modeled relation between fluorescent responses and blocker concentrations could be approximately fitted with the Hill equation to get EC_{50}. The EC_{50} acquired for specific compound does not have linear relation to the IC_{50} of the compound for blocking the channel activity in patch-clamp recording because the Hill slope of the dose-response curve for channel blockade determines the slope of the dose-response curve for

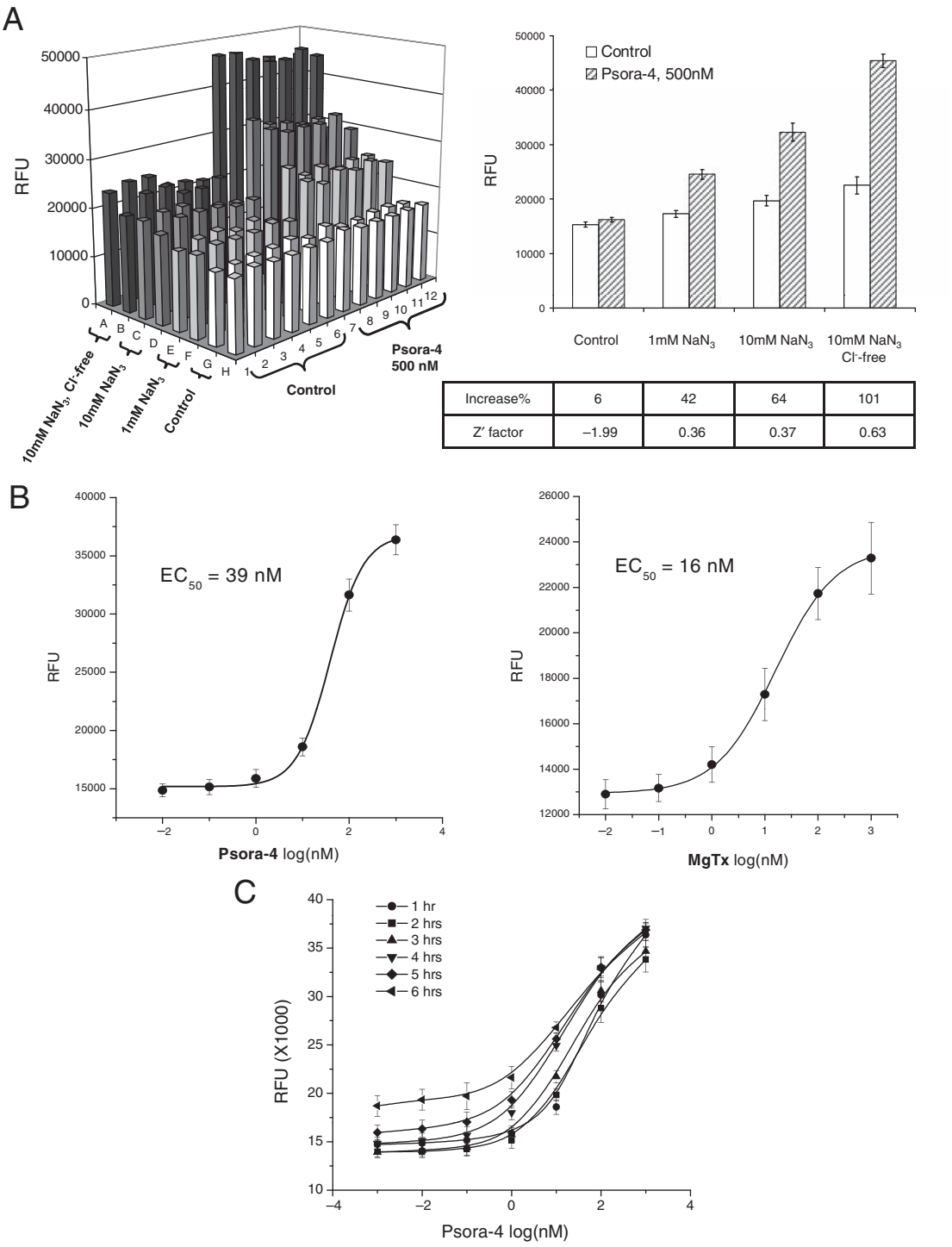

FIG. 3. Sodium azide in Cl^- free buffer dramatically increased the fluorometric imaging plate reader (FLIPR) assay window. (**A**) The plate view of Psora-4 effect in various conditions tested. The bar graph shown on the right summarizes the results from the plate (n = 12 for each group). (**B**) Dose response derived from FLIPR assay for Psora-4 and MgTx. Data were fitted with the Hill equation to obtain EC_{50} (n = 12 for each data point). (**C**) Assay performance showed in dose responses of the assay to Psora-4 within 1 to 6 h after dye loading of the cells. n = 12 for each data point.

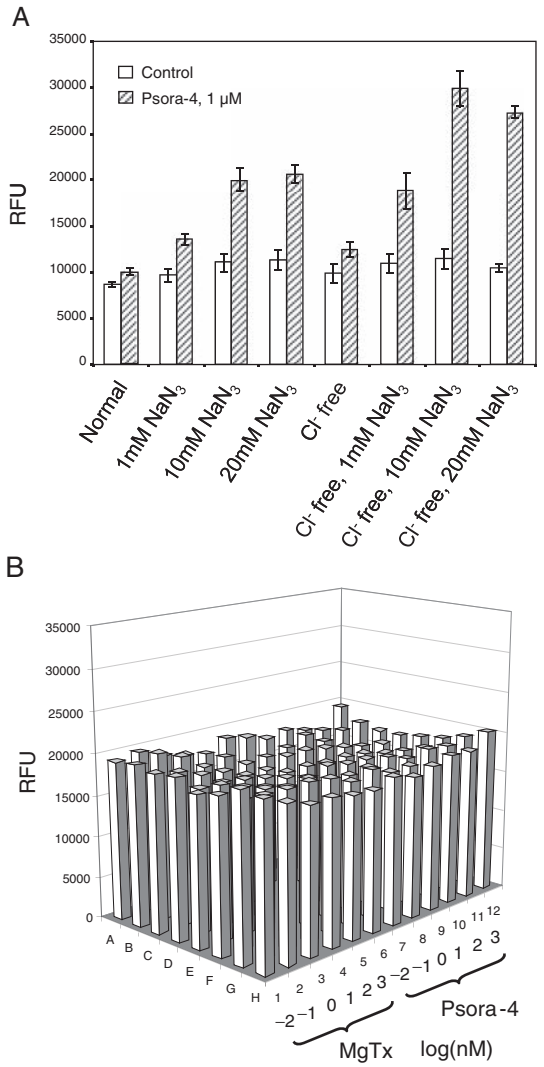

FIG. 4. Sodium azide in Cl^- free buffer significantly improved the fluorometric imaging plate reader (FLIPR) assay window for CHO-Kv1.5 but not Chinese hamster ovary (CHO) parental cells. (**A**) Fluorescence intensity from FLIPR assay on CHO-Kv1.5 cells in response to Psora-4 under various conditions (n = 6 for each group). (**B**) The plate view of the FLIPR results in response to Psora-4 and MgTx on CHO parental cells in the presence of 10 mM sodium azide in Cl^- free buffer.

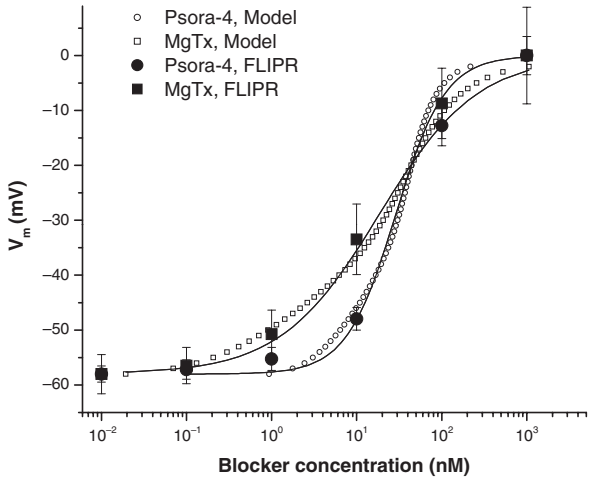

FIG. 5. Kinetic modeling of membrane potential as a function of blocker concentrations (see Materials and Methods). Presumably, Kv1.3 channel activation is the only mechanism to maintain membrane potential. As a result, effect of Psora-4 on membrane potential is illustrated in open circles using equation (3), where the parameters derived from patch-clamp recording (data not shown; see Vennekamp et al.[27]) are IC_{50} = 2 nM, G_0 = 50, V_K = –108 mV, k = 5.97, $V_{1/2}$ = –36.5 mV, and n = 2. For MgTx (open squares), IC_{50} = 0.2 nM and n = 1. The rest is same. The modeled voltage-concentration relation (equation 3) could be roughly fitted with the Hill equation (equation 2, solid line) to obtain EC_{50}. The experimental data acquired from the fluorometric imaging plate reader (FLIPR) assay were plotted into the graph (solid dots, n = 12 for each data point) after normalized to the minimal response at 10^{-2} nM of –58 mV and the maximal response at 10^3 nM of 0 mV.

membrane-potential modification. Psora-4 is known to have a Hill slope of 2 and MgTx has 1 for blocking channel activities.[27] The approximate fitting of the membrane-potential response results in 1.4 and 0.7 of the Hill slope, respectively. The EC_{50} of Psora-4 in FLIPR is 20-fold higher than its IC_{50} in patch clamp (39 vs. 2 nM), whereas MgTx has a 150-fold difference between these 2 parameters (16 vs. 0.11 nM).

Next, we conducted an HTS campaign for the Kv1.3 channel blockers using the FLIPR assay as described above. Single-point determinations were made on 650,000 compounds at 10 μM in around two thousand 384-well plates run over 17 days. We used 2 reference compounds in the control plates: Psora-4 and verapamil, a relatively less potent Kv1.3 blocker.[3,29] Both Psora-4 and verapamil induced a dose-dependent response in the control plate with average EC_{50}s of 150 nM and 3 μM, respectively. The Z′ robust factors, a good statistical measure for small populations, was derived from each test plate based on the high controls, 25 μM verapamil, and low controls, buffer-treated wells, indicating that the assay was reliable as most of the Z′ robust factors were greater than 0.6 (**Fig. 6A**) and a significant separation of the high controls and low controls was obtained (**Fig. 6B**). For those plates with Z′ factor less than 0.5 (88 of 2161), a retest was performed. The average Z′ robust in 2161 plates was 0.73, suggesting a statistically significant HTS assay. **Figure 6C** shows the results of the primary screen. The normal distribution analysis of the log fold induction (FI in logarithm scale) in fluorescence signal generated 3 times the interquartile range standard deviation (IQRSD) over the median (a well-accepted cutoff parameter) at 0.14 Log(FI) or 1.38 FI over buffer-treated wells. This cutoff value identified 20,948 compounds that were considered primary hits, a 3.2% hit rate. These hits were retested in triplicate at both 10 and 1

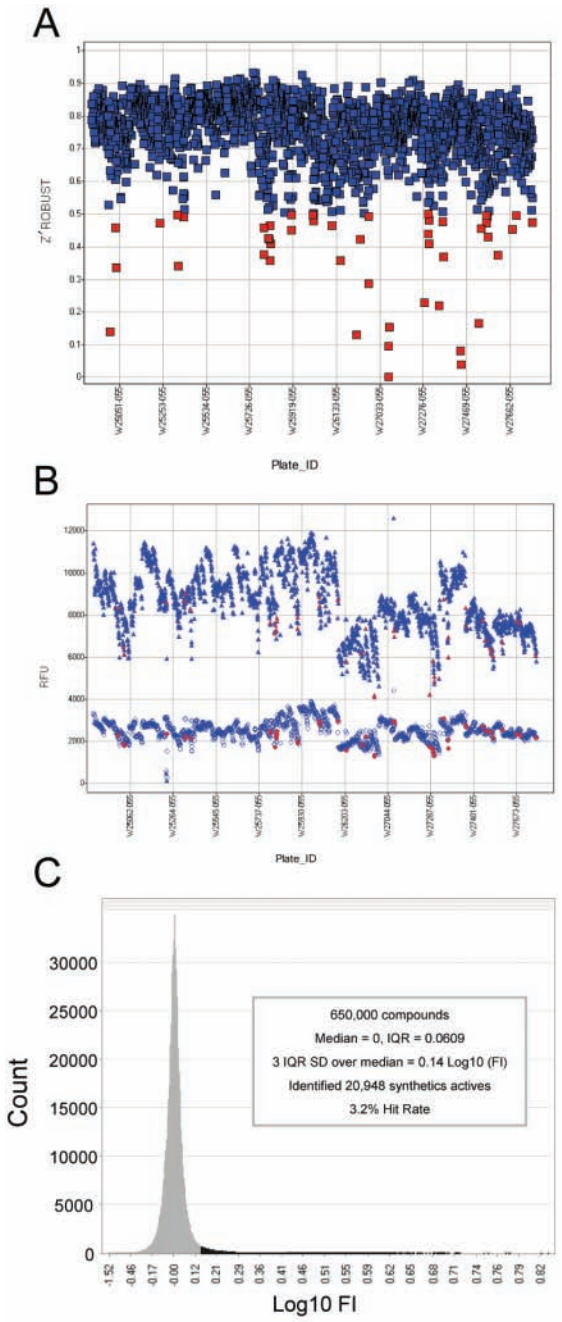

FIG. 6. Quality control of the assay and the results of the high-throughput screening (HTS). (**A**) Z′ robust values for each plate throughout the primary HTS campaign. The Z′ robust was calculated with buffer control as low signal ($n = 16$) and 25 μM verapamil as high signal ($n = 16$). (**B**) Medians of high controls and low controls for each plate throughout the primary HTS campaign. (**C**) Distribution of total compound activities in the HTS campaign represented as fold induction (FI) in logarithm scale. The compounds were tested at 10 μM. Based on the population statistics, the hit cutoff was set at 1.4 FI (3 times the interquartile range standard deviation [IQRSD] over the median), generating a 3.2% hit rate.

μM in the same procedure as the primary screen. Despite the statistical robustness of the controls throughout the HTS campaign, only 16% (3338 of 20,948) of the hits were confirmed to have a ≥1.38-fold increase based on the median of the triplicates. The vast majority of the hits that did not confirm were originally between the 3 IQRSD cutoff and 4 IQRSD over the median, as expected. However, more than one quarter of the confirmed actives came from retesting the hits in the 3 to 4 IQRSD range, justifying going deep into the normal distribution to find actives. We also conducted a counterscreen using parental CHO cells with the same assay procedure. This was a productive process that eliminated 3006 of the actives because they had either greater than 1.38 FI in the parental CHO cell line or a statistically insignificant difference in activity between the Kv1.3 and the parental CHO cells. The remaining 332 compounds were designated as high-quality hits, of which 258 compounds were moved to the next level of assessment because they had also demonstrated activity (≥1.38 FI) at 1 μM.

Our bench-top characterization of HTS hits was first performed on these 258 hits with the FLIPR dose-response assay. Most of the hits were active with EC_{50}s from 0.1 to 30 μM. Eight compounds were considered inactive hits with EC_{50}s greater than 60 μM. **Figure 7A** shows the correlation between EC_{50} and the percent increase in the HTS screen at 1 μM. Fifty-two compounds with EC_{50}s less than 1 μM were tested further in the automated patch-clamp IonWorks Quattro (Molecular Devices). Forty-seven compounds were potent blockers with IC_{50}s less than 1 μM. There was a significant linear correlation ($p < 0.001$) between EC_{50} in FLIPR and IC_{50} in IonWorks, as shown in **Figure 7B**. Chemical structure analysis indicated the discovery of diverse scaffolds. There were 31 singleton compounds with IC_{50}s ranging from single-digit nM to μM. Seven chemical classes with more than 1 compound in each class had sub-micromolar IC_{50}s (**Fig. 7C**). The most potent compound had the IC_{50} at nM range in IonWorks. As shown in Figure 7D, this compound (compound A) completely blocked the Kv1.3 channel current at the end of a 1-s pulse in IonWorks at 30 nM. In addition, in the presence of compound A, there was much less current induced by the second pulse after 1-s repolarization, suggesting that binding of compound A to the channel inhibited the recovery from the inactivation state.

We next characterized the lead compounds in patch-clamp recording. At least 2 types of blocking kinetics were identified. **Figure 8A,B** shows an example of use-dependent block, as compound B blocked the channel only when the channel was activated by depolarization pulses. In contrast, in **Figure 8C,D**, compound C blocked the channel regardless of the channel state, displaying a none-use-dependent blocking kinetics. These results demonstrate that the FLIPR membrane-potential assay developed in this study can be used to identify compounds with multiple blocking mechanisms for Kv1.3 channel blockers.

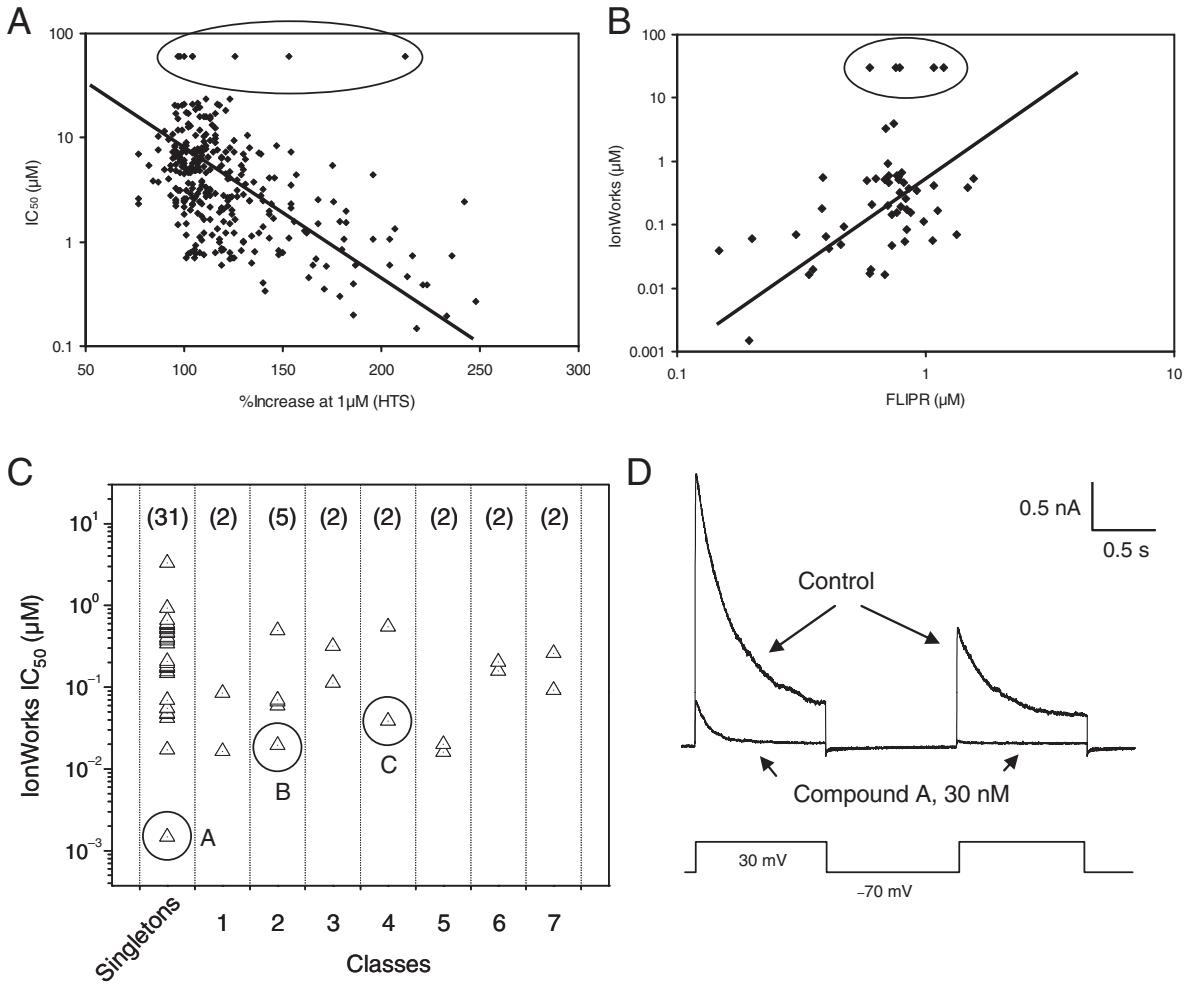

FIG. 7. Correlation of the compound activities across the different assays and the active compounds identified. (**A**) The EC_{50}s acquired by the fluorometric imaging plate reader (FLIPR) in the follow-up screen are plotted against the percent increase from the high-throughput screening (HTS) screen at 1 μM. The straight line represents linear fit to the equation described in Materials and Methods. The fitting parameters are as follows: a, 1.5; b, –0.01; *r* (correlation coefficient), –0.49; $p < 0.001$. (**B**) The IC_{50}s derived from IonWorks are plotted against the EC_{50}s from the FLIPR assay. The ovals indicate the compounds with the EC_{50} (or IC_{50}) exceeding the assay limit. The fitting parameters are as follows: a, –0.24; b, 1.98; *r*, 0.45; $p < 0.001$. (**C**) Selected compound potencies in multiple chemical classes. The numbers on top of the graph show the number of compounds in the class. Three compounds circled are used for the following figures as compounds A, B, and C. (**D**) Effect of compound A on Kv1.3 current in IonWorks evoked by a double-pulse voltage protocol.

In this article, we have described a robust assay to screen compounds for the blockers of voltage-gated K^+ channel Kv1.3. We successfully applied the assay to an HTS screen and the follow-up hit characterization. Membrane-potential assay to date is still a major assay format for assessment of K^+ channel activities. Physiologically, a number of K^+ channels function to modify resting membrane potential and to evoke downstream events thereafter. For such channels, the membrane-potential assay is more physiologically relevant and should be a more precise and direct way to assess the compound activities. On the other hand, using physiological buffer conditions for the assay would also shift the compound assessment toward physiologically relevant hits, reducing the number of nonspecific responders. However, expression cell lines do not show significant changes in membrane potential by blocking exogenously expressed K^+ channels, probably due to the endogenous membrane-potential maintaining mechanism. Particularly in CHO cells, ATP-dependent mechanisms help maintain membrane potential that could be effectively abolished by application of an inorganic compound, sodium azide. Removing extracellular chloride further boosted the membrane-potential signal, suggesting an involvement of a chloride

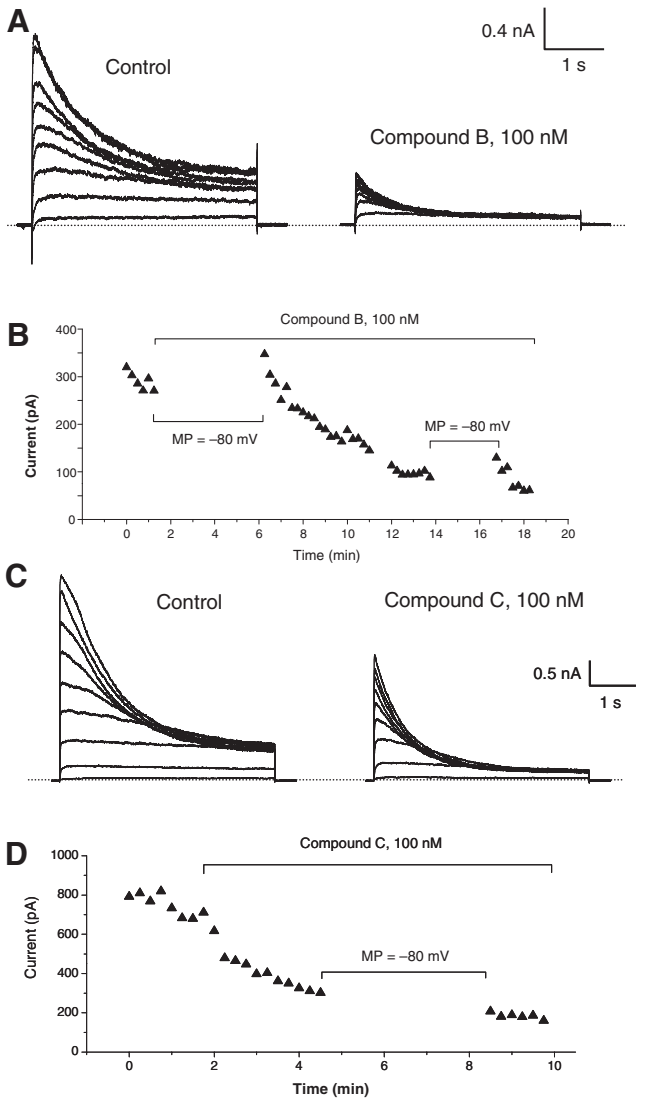

FIG. 8. Effect of compounds B and C on Kv1.3 current in patch-clamp recording. (**A**) Current recorded from a CHO-Kv1.3 cell before and after incubation of compound B at 100 nM. The voltage protocol contained a series of 3-s voltage pulses from –40 to 40 mV in increments of 10 mV. The holding potential was at –80 mV. (**B**) The time course of the effect shown in **A**. The current amplitude depicted at the end of a single pulse at 40 mV from –80 mV applied repetitively at a 15-s interval is plotted against time. The compound was perfused for 5 min at the holding membrane potential of –80 mV before reapplying the depolarizing pulses. During the second blank period, membrane potential was held at –80 mV. (**C**) Current recorded from a CHO-Kv1.3 cell before and after incubation of compound B at 100 nM. The voltage protocol was the same as in **A**. (**D**) The time course of the effect shown in **A**.

transporting system. In the optimal conditions described in this study, the Kv1.3 blocker-evoked signal could reach a good window, and the assay was robust with a Z′ factor acceptable for HTS. The functional model based on biophysical kinetics of the channel and effect of the reference compounds fit the experimental data very well, suggesting that in this cellular system under the developed conditions, the recombinant Kv1.3 channels are solely responsible for setting up membrane potential.

For assessment of ion channel activities, electrophysiological approaches are often used for validation of other assay formats. The data collected from the membrane-potential assay should be very well correlated with electrophysiology to be considered a robust assay. However, the model we established in this study suggests that the 2 assays may not generate results in good correlation as expected. Electrophysiology is measuring compound potency on ionic current across membrane, whereas the FLIPR assay is detecting membrane-potential change by ionic accumulation. Based on this model, EC_{50}s obtained from membrane-potential assay are much higher than the IC_{50}s from electrophysiology for the same compound. For the different compounds, IC_{50} or EC_{50} obtained from these 2 assays may not be linearly related if the compounds have different kinetic parameters such as the Hill coefficient (equation 3 and **Fig. 5**). This has been clearly demonstrated by the 2 example compounds, Psora-4 and MgTx, which block Kv1.3 channels with a different Hill coefficient in electrophysiology. Psora-4 has a 20-fold potency difference in the 2 assays, whereas MgTx shows a 150-fold potency difference. The data modeling provides a theoretical relationship between the 2 different assay formats and should be potentially useful in comparison and interpretation of experimental data. In addition, the results from the modeling suggest that under the physiological conditions, the K^+ channel blockers depolarize membrane potential much less potently than block K^+ channel current in patch-clamp settings. Highly potent compounds may be needed to modify membrane potential significantly in target tissues as therapeutic agents.

The assay we developed in this study should not be limited to their use for Kv1.3 channels. It could be reasonably applied for other Kv channels that have similar activation properties. We did examine CHO-hKv1.5 cells and found that the assay performed very well (**Fig. 4A**). The voltage-gated K^+ channels functioned independently of energy consumption. As one of the simplest chemical compounds, sodium azide can be an ideal agent to deplete intracellular ATP for assay simplicity. For many ion channels, depletion of ATP does not significantly modify channel activities. Sodium azide can be used in the assays for these channels if the intracellular ATP level is a concern for assay performance. For example, in the FLIPR Ca^{2+} channel assay using Ca^{2+} dye, the Ca^{2+} signal is often transient despite the continuous channel activation. The quick decline in Ca^{2+} signal is attributed to the subsequent activation of the Ca^{2+} excretion process. A significant part of this process is the Ca^{2+} pump located on the cell membrane and the intracellular Ca^{2+} store. By blocking the pump activity, inclusion of sodium azide into the assay buffer could significantly increase the signal

durability and the assay window (unpublished data). The assay performance can be largely improved. If properly designed, this approach is likely used in the assays for different types of membrane proteins, such as GPCR.

REFERENCES

1. Beeton C, Pennington MW, Wulff H, Singh S, Nugent D, Crossley G, et al: Targeting effector memory T cells with a selective peptide inhibitor of Kv1.3 channels for therapy of autoimmune diseases. *Mol Pharmacol* 2005;67:1369-1381.
2. Beeton C, Wulff H, Standifer NE, Azam P, Mullen KM, Pennington MW, et al: Kv1.3 channels are a therapeutic target for T cell-mediated autoimmune diseases. *Proc Natl Acad Sci USA* 2006;103:17414-17419.
3. Chandy KG, Wulff H, Beeton C, Pennington M, Gutman GA, Cahalan MD: K^+ channels as targets for specific immunomodulation. *Trends Pharmacol Sci* 2004;25:280-289.
4. Grissmer S, Dethlefs B, Wasmuth JJ, Goldin AL, Gutman GA, Cahalan MD, et al: Expression and chromosomal localization of a lymphocyte K^+ channel gene. *Proc Natl Acad Sci USA* 1990;87:9411-9415.
5. Hu L, Pennington M, Jiang Q, Whartenby KA, Calabresi PA: Characterization of the functional properties of the voltage-gated potassium channel Kv1.3 in human CD4+ T lymphocytes. *J Immunol* 2007;179:4563-4570.
6. Wulff H, Calabresi PA, Allie R, Yun S, Pennington M, Beeton C, et al: The voltage-gated Kv1.3 K^+ channel in effector memory T cells as new target for MS. *J Clin Invest* 2003;111:1703-1713.
7. Wulff H, Pennington M: Targeting effector memory T-cells with Kv1.3 blockers. *Curr Opin Drug Discov Devel* 2007;10:438-445.
8. Desir GV: Kv1.3 potassium channel blockade as an approach to insulin resistance. *Expert Opin Ther Targets* 2005;9:571-579.
9. Xu J, Wang P, Li Y, Li G, Kaczmarek LK, Wu Y, et al: The voltage-gated potassium channel Kv1.3 regulates peripheral insulin sensitivity. *Proc Natl Acad Sci USA* 2004;101:3112-3117.
10. Behrendt HJ, Germann T, Gillen C, Hatt H, Jostock R: Characterization of the mouse cold-menthol receptor TRPM8 and vanilloid receptor type-1 VR1 using a fluorometric imaging plate reader (FLIPR) assay. *Br J Pharmacol* 2004;141:737-745.
11. Benjamin ER, Skelton J, Hanway D, Olanrewaju S, Pruthi F, Ilyin VI, et al: Validation of a fluorescent imaging plate reader membrane potential assay for high-throughput screening of glycine transporter modulators. *J Biomol Screen* 2005;10:365-373.
12. Smart D, Jerman JC, Gunthorpe MJ, Brough SJ, Ranson J, Cairns W, et al: Characterisation using FLIPR of human vanilloid VR1 receptor pharmacology. *Eur J Pharmacol* 2001;417:51-58.
13. Sullivan E, Tucker EM, Dale IL: Measurement of $[Ca^{2+}]$ using the fluorometric imaging plate reader (FLIPR). *Methods Mol Biol* 1999;114:125-133.
14. Trivedi S, Dekermendjian K, Julien R, Huang J, Lund PE, Krupp J, et al: Cellular HTS assays for pharmacological characterization of $Na_v1.7$ modulators. *Assay Drug Dev Technol* 2008;6:167-179.
15. Vickery RG, Amagasu SM, Chang R, Mai N, Kaufman E, Martin J, et al: Comparison of the pharmacological properties of rat $Na_v1.8$ with rat $Na_v1.2a$ and human $Na_v1.5$ voltage-gated sodium channel subtypes using a membrane potential sensitive dye and FLIPR. *Receptors Channels* 2004;10:11-23.
16. Wolff C, Fuks B, Chatelain P: Comparative study of membrane potential-sensitive fluorescent probes and their use in ion channel screening assays. *J Biomol Screen* 2003;8:533-543.
17. Zhang Y, Kowal D, Kramer A, Dunlop J: Evaluation of FLIPR Calcium 3 Assay Kit—a new no-wash fluorescence calcium indicator reagent. *J Biomol Screen* 2003;8:571-577.
18. Gill S, Gill R, Wicks D, Liang D: A cell-based Rb^+-flux assay of the Kv1.3 potassium channel. *Assay Drug Dev Technol* 2007;5:373-380.
19. Jorgensen S, Johansen TH, Dyhring T: Fluorescence-based Tl^+-influx assays as a novel approach for characterization of small-conductance Ca^{2+}-activated K^+ channel modulators. *Methods Mol Biol* 2008;491:257-266.
20. Weaver CD, Harden D, Dworetzky SI, Robertson B, Knox RJ: A thallium-sensitive, fluorescence-based assay for detecting and characterizing potassium channel modulators in mammalian cells. *J Biomol Screen* 2004;9:671-677.
21. Whiteaker KL, Gopalakrishnan SM, Groebe D, Shieh CC, Warrior U, Burns DJ, et al: Validation of FLIPR membrane potential dye for high throughput screening of potassium channel modulators. *J Biomol Screen* 2001;6:305-312.
22. Ebneth A, Netzer R, Hahn U: Method for examining the activity of ion channels. United States Patent, 2007, US20070281330 A1.
23. Slack M, Kirchhoff C, Moller C, Winkler D, Netzer R: Identification of novel Kv1.3 blockers using a fluorescent cell-based ion channel assay. *J Biomol Screen* 2006;11:57-64.
24 Soloveva V, LaRocque J, McKillip E: When robots are good: fully automated thermo LAS robotic assay system with dual FLIPR Tetra and TAP SelecT robotic cell culture system. *JALA* 2006;11:145-156.
25. Gill S, Gill R, Wicks D, Despotovski S, Liang D: Development of an HTS assay for Na^+, K^+-ATPase using nonradioactive rubidium ion uptake. *Assay Drug Dev Technol* 2004;2:535-542.
26. Gribble FM, Loussouarn G, Tucker SJ, Zhao C, Nichols CG, Ashcroft FM: A novel method for measurement of submembrane ATP concentration. *J Biol Chem* 2000;275:30046-30049.
27. Vennekamp J, Wulff H, Beeton C, Calabresi PA, Grissmer S, Hansel W, et al: Kv1.3-blocking 5-phenylalkoxypsoralens: a new class of immunomodulators. *Mol Pharmacol* 2004;65:1364-1374.
28. Garcia-Calvo M, Leonard RJ, Novick J, Stevens SP, Schmalhofer W, Kaczorowski GJ, et al: Purification, characterization, and biosynthesis of margatoxin, a component of *Centruroides margaritatus* venom that selectively inhibits voltage-dependent potassium channels. *J Biol Chem* 1993;268:18866-18874.
29. Rauer H, Grissmer S: Evidence for an internal phenylalkylamine action on the voltage-gated potassium channel Kv1.3. *Mol Pharmacol* 1996;50:1625-1634.

Address correspondence to:
Kun Liu, Ph.D.
Department of Screening Sciences, Wyeth Research
500 Arcola Road, Collegeville, PA 19426

E-mail: liuk2@wyeth.com